SCHOOL OF ADVANCED TECHNOLOGY

SAT301 FINAL YEAR PROJECT

Design of a 60 GHz Band Patch Antenna Array for Vital Signs Monitoring Based on Doppler Radar Principles

Final Thesis

In Partial Fulfillment

of the Requirements for the Degree of

Bachelor of Engineering

Student Name	:	Jiaqi Yang
Student ID	:	2036578
Supervisor	:	Zhao Wang
Assessor	:	Jingchen Wang

Abstract

This project explores ultra-wide patch antenna arrays operating in the 60 GHz band (60-64 GHz) to remotely detect human respiratory and heartbeat frequencies using Doppler radar principles, aiming at increased gain and beamwidth. The goal is to accurately measure the respiratory rate (BR) and heart rate (HR) at different distances from 30 to 150 mm in both single and dual antenna configurations. In the single-antenna setup, the same antenna is used to transmit and receive signals. In contrast, a dual-antenna setup uses two identical antennas, one for transmitting and the other for receiving. The aim of this study was to compare the accuracy and detection range of remote vital signs monitoring (RVSM) under single-antenna and dual-antenna operation, and to investigate the effect of increasing the number of patch elements on these parameters.

Keywords：

Microstrip antenna; Ultra-wide patch arrays; Remote vital sign monitoring; Doppler radar; Non-contact vital signs monitoring; 60 GHz antenna arrays

Acknowledgements

I would like to extend my deepest gratitude to my supervisor, Professor Zhao Wang, for her invaluable help and support, which was crucial to the successful completion of the FYP project. Many of her suggestions were of great help to me in overcoming the challenges encountered during the CST simulation. I am also grateful to Prof. Jingchen Wang for teaching me how to use the CST software, providing a solid foundation for my project work.

I am profoundly thankful to my parents for their unwavering trust and financial support, which allowed me to focus entirely on my studies and work without concern.

I am also very grateful to XJTLU for allowing me to pursue my studies and for the abundant resources and support throughout my academic journey. I also sincerely appreciate my friends' encouragement, companionship, and understanding during my studies.

Contents

List of Tables

List of Figures

List of Acronyms

FMCW	Frequency Modulated Continuous Wave
RVSM	Remote Vital Signs Monitoring
WPANs	Wireless Personal Area Networks
WLANs	Wireless Local Area Networks
WMANs	Wireless Metropolitan Area Networks
PAAs	Phased Array Antennas
MIMO	Multiple Input Multiple Output
SIW	Substrate Integrated Waveguide
VR	Virtual Reality
AR	Augmented Reality
IoT	Internet of Things
DRS	Doppler Radar Sensors
BR	Breathing Rate
HR	Heart Rate
VMD	Variable Mode Decomposition

Chapter 1

Introduction

1.1 Background

In recent years, there has been a rise in interest in creating non-contact techniques for tracking vital signs, including heart and breathing rates, due to the rapid advancements in healthcare technology [1]. Traditional methods of vital signs monitoring limit the ability to continuously and non-invasively monitor an individual's health due to their painful contact nature [2]. The 60 GHz frequency band was chosen for this study because of its broad bandwidth and high resolution, which allows for more accurate and high-end collection of basic physiological information. The Doppler radar technology adopted by this technology system is capable of making accurate measurements, especially in capturing weak physiological signals such as heartbeat and respiration [3]. Given that its 60 GHz frequency covers the range between 57-66 GHz, no additional authorisation certificates are required for the use of this technology, and it is already widely used in a number of wireless services, it is particularly suitable for these specific applications [4]. 60 GHz operating systems have made significant advances, but there are still numerous issues that need to be resolved, such as degradation and transmission of electromagnetic waves, data misreporting of fast-moving data misreporting from fast moving objects, energy efficiency and thermal regulation. It is crucial to overcome these difficulties and build a stable and efficient touchless vital signs detection system.

1.2 Project Description

1.2.1 General View of the Project:

We conducted research for this project focusing on touchless pulse and heartbeat monitoring at the wrist. The key reasons behind the selection of Doppler Radar Sensors (DRS) include their privacy-protecting features, their ability to adapt to a variety of lighting environments, and their non-touchable nature [14]. Doppler radar technology offers a more practical and efficient method for vital signs detection than surveillance devices used to observe skin contact [14]-[22]. This project also highlights the general application of small, low-cost, lightweight millimetre-wave Doppler radar systems in the field of remote vital signs monitoring (RVSM) [23]-[26].

1.2.2 Importance of the Project:

I chose to explore this project in depth because the need for non-contact vital sign monitoring in the broad areas of healthcare, security and defence is growing [15]-[22]. I chose to use Doppler radar sensors to drive this project because of the technology's non-intrusive nature, its ability to adapt to multiple light conditions, and its privacy benefits, among many other advantages [14]. Doppler radar systems are easier to use than traditional surveillance tools, consume less energy, and have significantly shorter start-up times [15]-[22]. The use of millimetre wave frequencies combined with an array of antennas can effectively reduce interference and improve detection accuracy [27]-[30]. The main focus of this project is to develop radar systems that are more cost effective, energy efficient and efficiently integrated. By incorporating these systems into modern portable tools such as tablet computers and smartphones, we can drive technological innovation [32]. In short, this research is critical to the advancement of non-contact vital signs monitoring, which has the potential to be applied in many fields and is also of immense value to the evolution of healthcare safety technology.

1.3 Motivation, Aims and Objective

Problems Description:

Conventional vital signs monitoring systems often result in uncomfortable physical contact with people, which makes it tricky to monitor people's health in a continuous and non-invasive manner. Currently, non-contact vital signs monitoring systems are facing a number of difficulties, including the gradual attenuation and transmission of electromagnetic waves, motion artefacts, efficient energy consumption, and heat management in 60 GHz systems.

Motivation:

As healthcare technology continues to advance, the importance of non-contact detection of vital indicators such as heart rate and respiratory rate is becoming more and more popular. Utilising the 60 GHz spectrum allows for superior resolution and bandwidth, resulting in more accurate and comprehensive vital sign data collection. The aim of this research is to utilise the concept of Doppler radar to obtain accurate and specific velocity detection values. This series of data is particularly important for tracing subtle signs in physiology.

Aims:

Addressing the challenges of Remote Vital Signs Monitoring (RVSM) has become the primary goal in this project. In order to further improve performance over a diverse frequency range, our initial vision was to create an array of microstrip antennas containing three ultra-wideband components, each incorporating specific patch elements based on a unique design. In addition to this, we have the intention of evaluating the operational efficiency of a Remote Vital Signs Monitoring (RVSM) system using both single-antenna and dual-antenna systems, with a particular focus on the detection range and accuracy of the system. This project also plans to test and analyse the system in a number of different scenarios in order to accurately assess the capability of vital signs screening as well as to determine the longest range settings for the various configurations.

We will delve into the functionality of the various components within the antenna array and pay special attention to the potential pitfalls that these components may pose to the accuracy and coverage of the detection. Our various experimental studies and in-depth discussions provide valuable research references for improving the performance and outcomes of remote vital signs monitoring systems.

Objectives:

1. Design of three ultra-wide element microstrip antenna arrays with 6×1, 3×2 and 6×2 patch elements.

2. Ensure that the reflection coefficient of the system is below -10 dB in the 60-64 GHz band so that the antenna can absorb or transmit the signal effectively.

3. To evaluate the effectiveness of the antenna design, observe the antenna's ability to reflect signals at different distances

1.4 Literature Review

A. Development history and Present status of development

Exploration of the 60 GHz band commenced in the early 1990s as individuals started to acknowledge the possible uses of this frequency range. Scientists have initiated the development and examination of antennas and RF front-end technology that are designed explicitly for the 60 GHz frequency spectrum [5]. The IEEE released the 802.15.3c standard in 2009, which designates the 60 GHz spectrum for Wireless Personal Area Network (WPAN) communications. As a result, there was a subsequent increase in the thorough investigation and advancement of antenna technology, specifically in the 60 GHz frequency band [6]. Currently, the 60 GHz spectrum is extensively utilized in high-speed wireless communications. Existing patch antenna arrays operating at 60 GHz, now available in the market, typically comprise numerous antenna units placed compactly to enhance communication performance by extending the range for receiving and transmitting signals. These patch antenna arrays are usually compact and lightweight and are particularly suitable for integrating into embedded systems and mobile devices. In addition, according to reference [7], significant

progress has been made in developing 60 GHz patch antenna arrays, where the antenna gain has been enhanced and the beamwidth has been reduced. This means they can achieve more robust signal transmission and excellent interference immunity, thus improving communication quality and stability.
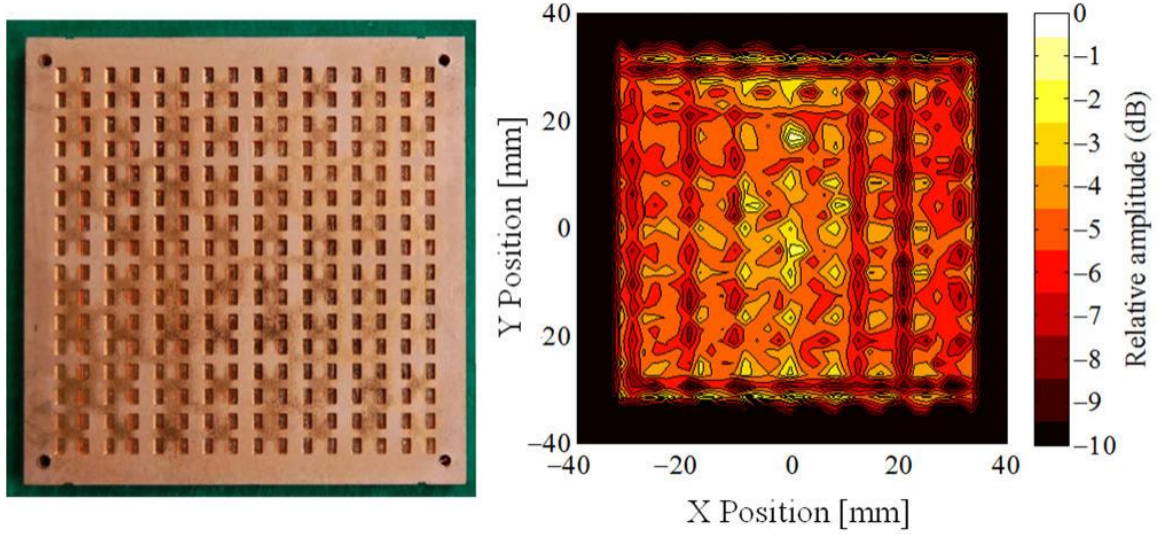

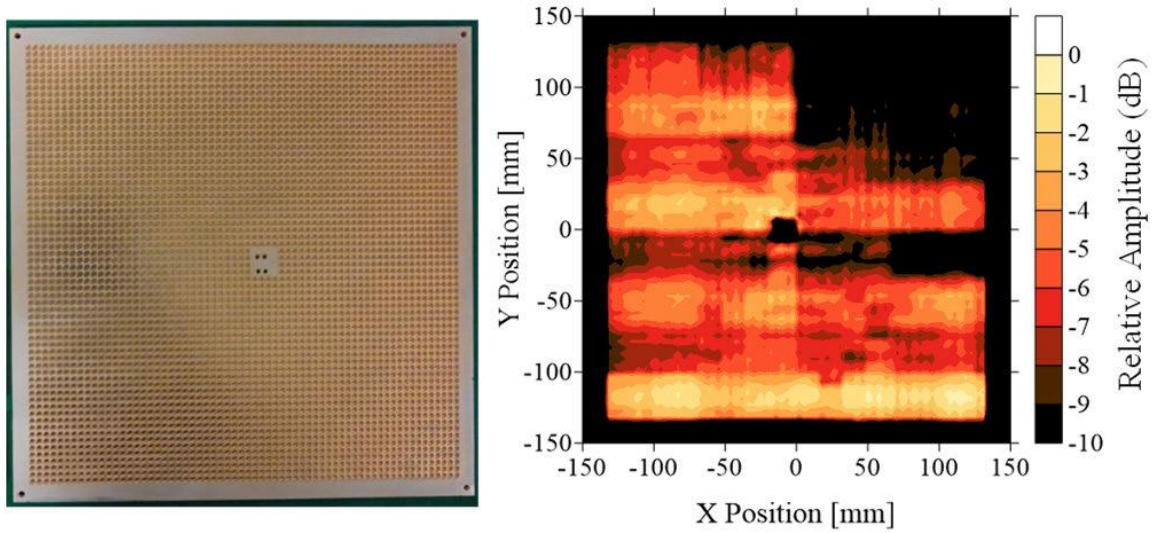Fig. 1. Photographs and aperture distributions of the 16×16 [7]

Fig. 2. Photographs and aperture distributions of the 64×64 [7]

B. Application Necessity

In the frequency band of 60 GHz, the array of antennas is widely used in several fields and at the same time it plays an indispensable effect.

First of all, the arrangement of antennas in this band helps in the high speed transmission of data.The bandwidth of 60 GHz is very wide and the speed and size of data transmission can be significantly enhanced by using such antenna arrays [8], so this technique is highly favoured in data-intensive application scenarios such as wireless communication, high-definition video transmission, virtual reality as well as augmented reality.

In addition to this, an array of antennas at 60 GHz frequency can also be used as a tool for fast wireless connectivity. Wireless Local Area Networks (WLANs) and Wireless Metropolitan Area Networks (WMANs) are regarded as examples of high-speed, stable broadband wireless Internet, which, thanks to their high-frequency attributes, allow for the construction of faster and more reliable signal propagation [9].

These antenna arrays are also suitable for millimetre wave radar application scenarios. Due to the wavelength properties of millimetre waves, radar systems are able to achieve higher clarity and more precise target exploration [8]. The antenna arrays are able to perform deeper and more precise radar measurements in the 60 GHz band, a feature that has significant utility in a number of fields such as security monitoring, target tracking, and unmanned vehicles

C. Challenges and corresponding solutions

Antenna arrays at 60 GHz bandwidth enable short-range, high-speed wireless communications, such as wireless personal area networks (WPANs) and fixed and mobile access networks [10], [11]. Since WPANs require phased array antennas (PAAs) with high gain and wide coverage area, measurements of PAAs require three-dimensional characterization of their radiation patterns. However, two-dimensional measurements are usually used due to the limitations of the measurement system. In

[10], to mitigate the mutual coupling among the element antennas, a monolithic microwave integrated circuit (MMIC) is integrated onto the feed line of each element antenna.
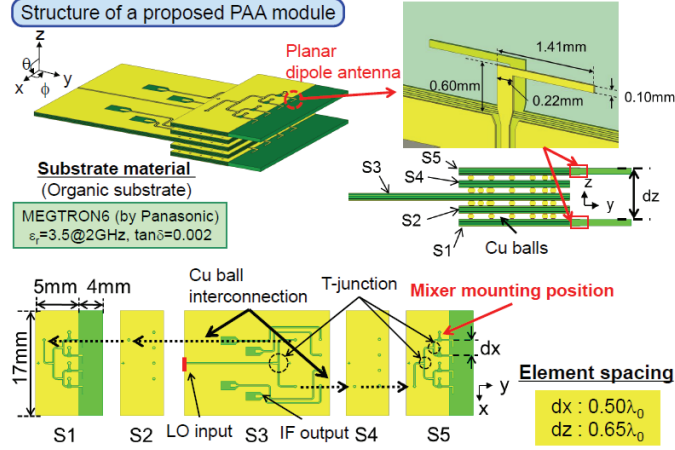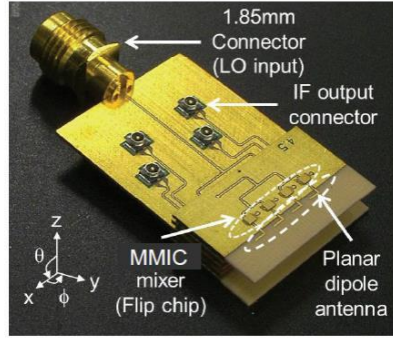

Fig. 3. Structure of fabricated 2 x 4 PAA module [10]

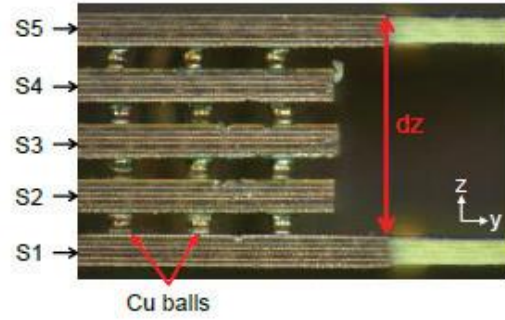

Fig. 4. Fabricated 4 × 2 dipole antenna array [10]

Fig. 5. Side view of PAA module [10]

In [11], an optimized solution for 60 GHz Multiple Input Multiple Output (MIMO) antennas is proposed to reduce the mutual coupling between antennas for Wireless Personal Area Network (WPAN) applications. A pair of folded L-shaped strip patches are used, and the antenna performance is improved by adding a tapered ground-blocking structure.
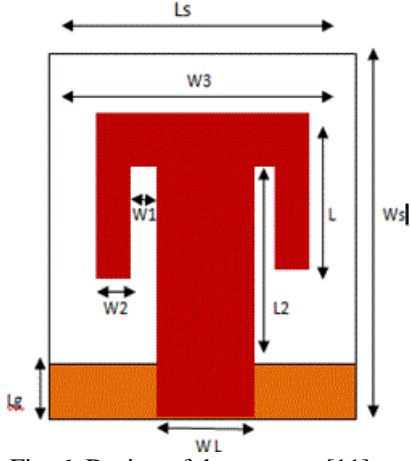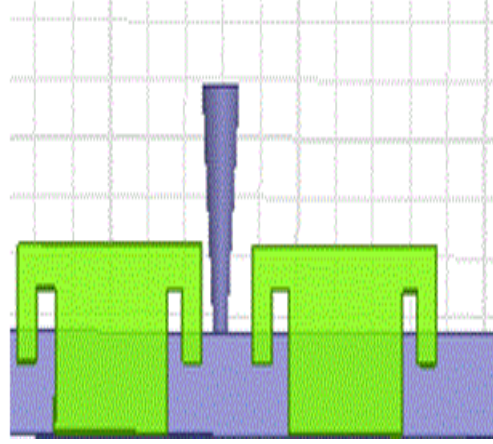
Fig. 6. Design of the antenna [11]

Fig. 7. Layout of multiple antenna systems with the ground stub [11]

The difficulty of fabricating antennas has been a barrier to antenna development. In [12], the total number of dielectric layers was reduced to two by integrating the feed circuit and the radiating waveguide into a single dielectric layer, significantly increasing the difficulty of mass production.
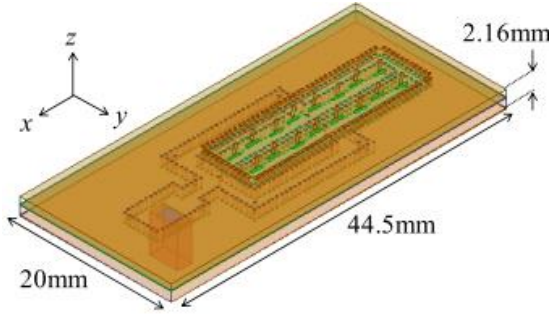
Fig. 8. The analysis of the full structure [12]
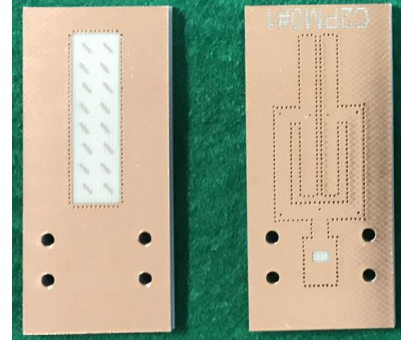
Fig. 9. The fabricated antennas [12]

Conventional three-dimensional antennas are unsuitable for user terminals, so a planar multisector antenna design with a low profile and suitable for user terminals is proposed [13]. The article details the antenna design for the 60 GHz band using the Substrate Integrated Waveguide (SIW) technique [13]. It is mentioned that in order to achieve broadband and desired gain, a unique structure is used where multiple slit

elements are closely spaced, and the length of the slit increases from the short waveguide end to the feed end [13].
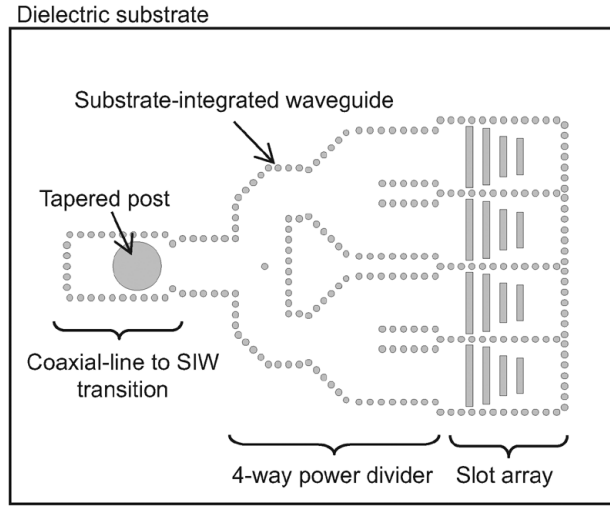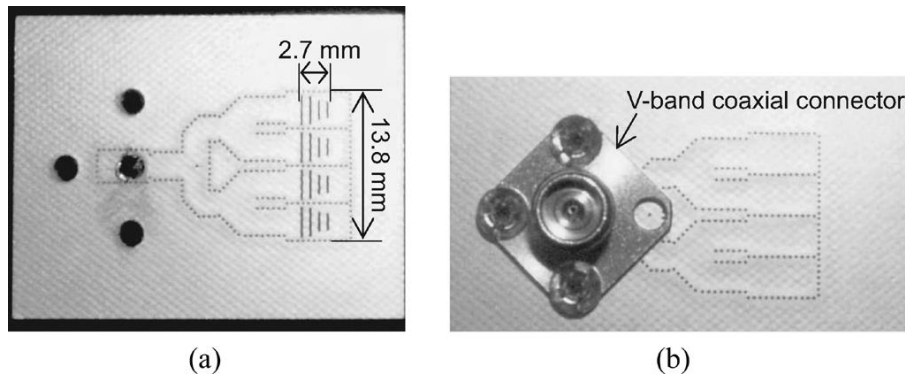

Fig. 10. The fabricated antennas [13]

Fig. 11. Fabricated slot array antenna. (a) Top and (b) bottom views [13]

Overall, there are many challenges regarding 60 GHz band antenna arrays, and as technology advances, these challenges will be solved. The following table is a summary of the challenges and solutions mentioned above:

Table. 1. Summary of the challenges and solutions

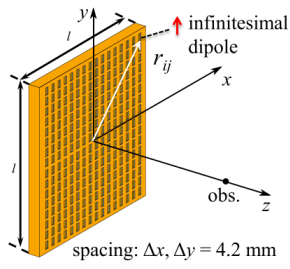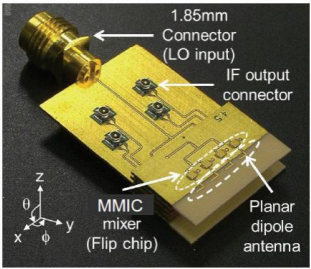| Challenge	Solution
Limited measurement system for two-dimensional measurements	Implementation of monolithic microwave integrated circuits (MMICs) on the feed line of each element antenna to reduce mutual coupling [10].
Mutual coupling between antennas in 60 GHz MIMO applications [11]	Adoption of a pair of folded L-shaped strip patches and the addition of a tapered ground blocking structure to optimize 60 GHz MIMO antennas for Wireless Personal Area Network (WPAN) applications [11].
Fabrication difficulty due to the total number of dielectric layers [12]	Integrating the feeder circuits and radiating waveguides into one dielectric layer reduces the total number of dielectric layers to two [12].
Unsuitability of conventional three-dimensional antennas for user terminals [13]	Proposal of a planar multisector antenna design using Substrate Integrated Waveguide (SIW) technique for user terminals at 60 GHz [13].
Need for broadband and desired gain in the planar multisector antenna [13]	Utilization of a special structure with closely spaced multiple slit elements and varying slit lengths from the short waveguide end to the feed end [13].

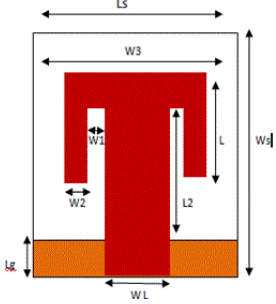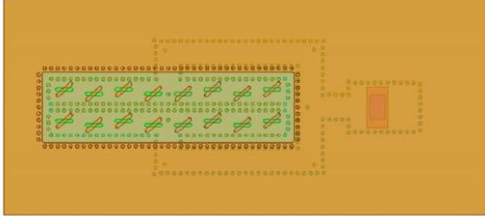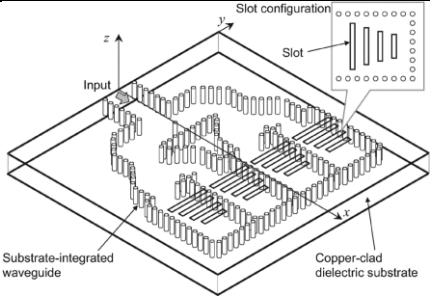## D. Prospects for patch antenna arrays in the 60 GHz band

Patch antenna arrays have great potential in the 60 GHz band, especially in high-speed wireless communications. Their compact planar design makes them ideal for integration into size-critical devices. The directional beamforming capability of patch

antenna arrays facilitates focused, efficient transmission to support applications such as point-to-point communication links. Utilizing millimeter-wave characteristics, these antennas enable wide bandwidth, meeting the demand for high-capacity data transmission in emerging technologies such as 5G. In addition, integrating these antennas into phased array systems enables electronic beam steering, improving adaptability to changing communication requirements. 60 GHz frequency band is susceptible to atmospheric absorption and signal fading, which can be mitigated by beamforming techniques to improve reliability. As a result, patch antenna arrays are expected to play a vital role in the evolving field of wireless communications technology, facilitating emerging use cases ranging from high-speed data transmission to wireless virtual reality (VR), augmented reality (AR) and Internet of Things (IoT) connectivity.

In conclusion, more types of antennas need to be continually investigated for use in the 60 GHz band. The following table is a summary of the antennas mentioned above:

Table. 2. Summary of the antennas mentioned

Reference	Structure	Antenna Type
[7]		N × N-element slot array antenna with uniform distribution.
[10]		Planar dipole array antenna

[11]		Patch antenna. The antenna is made of a pair of folded L-shaped strip patches on a silicon substrate
[12]		Broadband antenna based on Substrate-Integrated-Waveguide (SIW) and slotted arrays for building planar multi-sector antennas in the 60 GHz band.
[13]		Broadband substrate-integrated waveguide slot arrays based on slot elements.

Chapter 2

Methodology

2.1 Key parameters for Radar Antennas

The following are the structural diagrams and parameter values of the three microstrip patch antenna arrays:
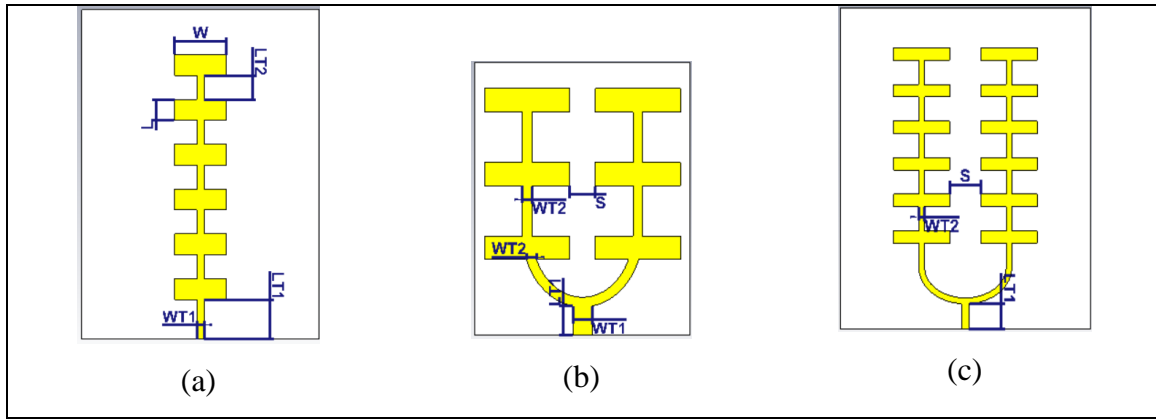
Fig. 12. Designed antenna array structure with (a) 6×1, (b) 3×2 and (c) 6×2 patch elements

The formulas for each parameter are as follows:

$W = \frac{\lambda_0(2M+1)}{2\sqrt{\frac{\varepsilon_r+1}{2}}}$, where M=1 and N=0

$L = \frac{\lambda_g(2N+1)}{2\sqrt{\varepsilon_{reff}}} - 2\Delta L$,

$L_{T1} = (2P + 1) \times \frac{\lambda}{4}$, where P=1.

$L_{T2} = \frac{\lambda_g}{2} + 2\Delta L$,

$S = \frac{\lambda_g}{2}$,

$W_{T1} = \frac{59.81\lambda_0}{n \times Z_a}$, where Z_a is the total input impedance and n is the number of symmetrical patch elements.

$W_{T2} = \frac{7.475h}{e^x} - 1.25t$, where $x = \frac{Z\sqrt{\varepsilon_r + 1.41}}{87}$ and t is copper cladding.

2.2 FMCW

FMCW stands for Frequency Modulated Continuous Wave. It is a modulation technique commonly used in radar systems. In FMCW radar, the frequency of the transmitted continuous wave varies linearly with time, and this variation is continuous and periodic. FMCW can detect the distance and velocity of an object by using radar, as well as small displacements of the object [42]. The basic form is：

$$s(t) = \exp\left(j2\pi\left(f_0 t + \frac{1}{2}kt^2\right)\right)$$

Where s(t) indicates the transmitted signal as a function of time t, f_0 is the starting frequency, k is the frequency sweep rate (the rate of frequency modulation over time), and j represents the imaginary unit.

The complex signal can be decomposed into real and imaginary parts, and the FMCW signal can also be written in the following form:

$$s(t) = \cos\left(2\pi\left(f_0 t + \frac{1}{2}kt^2\right) + \emptyset_0\right) + j\sin\left(2\pi\left(f_0 t + \frac{1}{2}kt^2\right) + \emptyset_0\right)$$

The following figure shows the FMCW signal written in MATLAB:
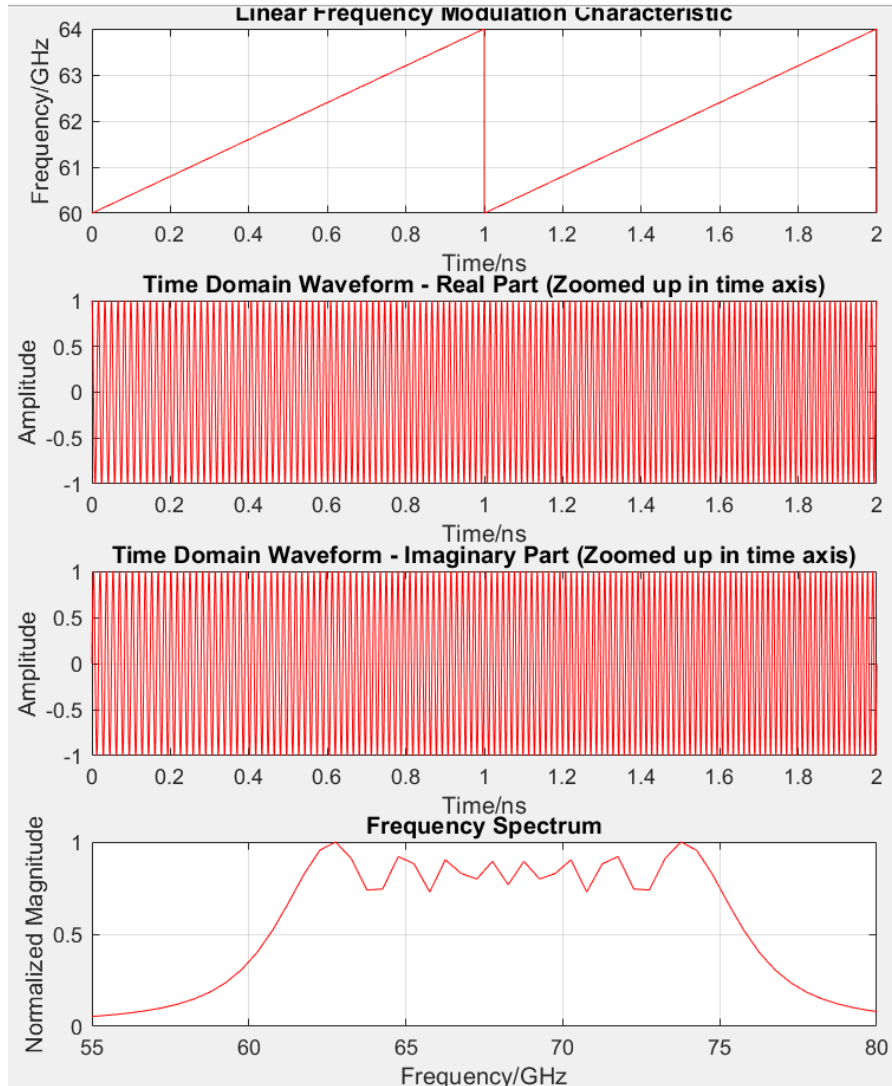
Fig. 13. FMCW

The "Linear Frequency Modulation Characteristics" section demonstrates the linear increase in signal frequency over time, from 60 GHz to 64 GHz, spanning from 0 to 2 nanoseconds. This linear variation is a crucial characteristic of Frequency Modulated Continuous Wave (FMCW) radars, allowing the radar to determine a target's distance and speed accurately. The time-domain waveform in the natural part depicts the temporal variation of the fundamental components of the signal. Due to the intricate nature of this signal, its actual component is depicted as a sinusoidal waveform. The waveform in the figure exhibits an amplitude that fluctuates between +1 and -1, which signifies the intensity

15

or magnitude of the signal's voltage. The time domain waveform displays the signal's imaginary component. Due to the complexity of the signal, the imaginary part also displays a sinusoidal waveform. The phase difference between the imaginary and actual parts is typically 90 degrees, indicating quadrature. The lower graph displays the signal's frequency spectrum, representing the signal in the frequency domain. The frequency spectrum depicts the allocation of signal energy across different frequencies. The graph clearly illustrates that the primary signal energy is focused inside the frequency range of 60 GHz to 75 GHz, which aligns with the linear frequency modulation characteristics mentioned before.

2.3 Simulation and Measurement Setup

The design is usually simulated using CST STUDIO SUITE, which is an electromagnetic simulation software. In this part, the simulation and measurement setup of 3×2 antenna arrays will be introduced in detail.

The following shows the feeding structure and related values of the antenna:
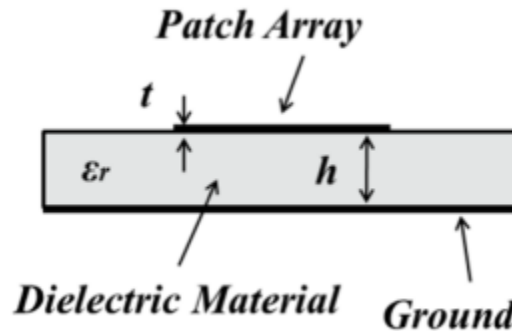
Fig. 14. Feeding structure

Table. 3. Data sheet for feeding structure

Dielectric constant (ε_r)	4.4
Thickness of substrate (h)	0.254mm
Thickness of conductor (t)	0.035mm

The specific parameters and values of this antenna are shown below:

Table. 4. The specific parameter values

	L	L$_{T1}$	LT2	W	WT1	WT2	S
Ant. 2	1.45	1.74	3.11	5.28	1.20	0.60	1.58

At the end of the simulation, looking at the S1,1 parameter it was found that it did not go below -10 dB at 60-64 GHz. Thus, the parameter needs to be optimized and this step can be done using the optimizer:
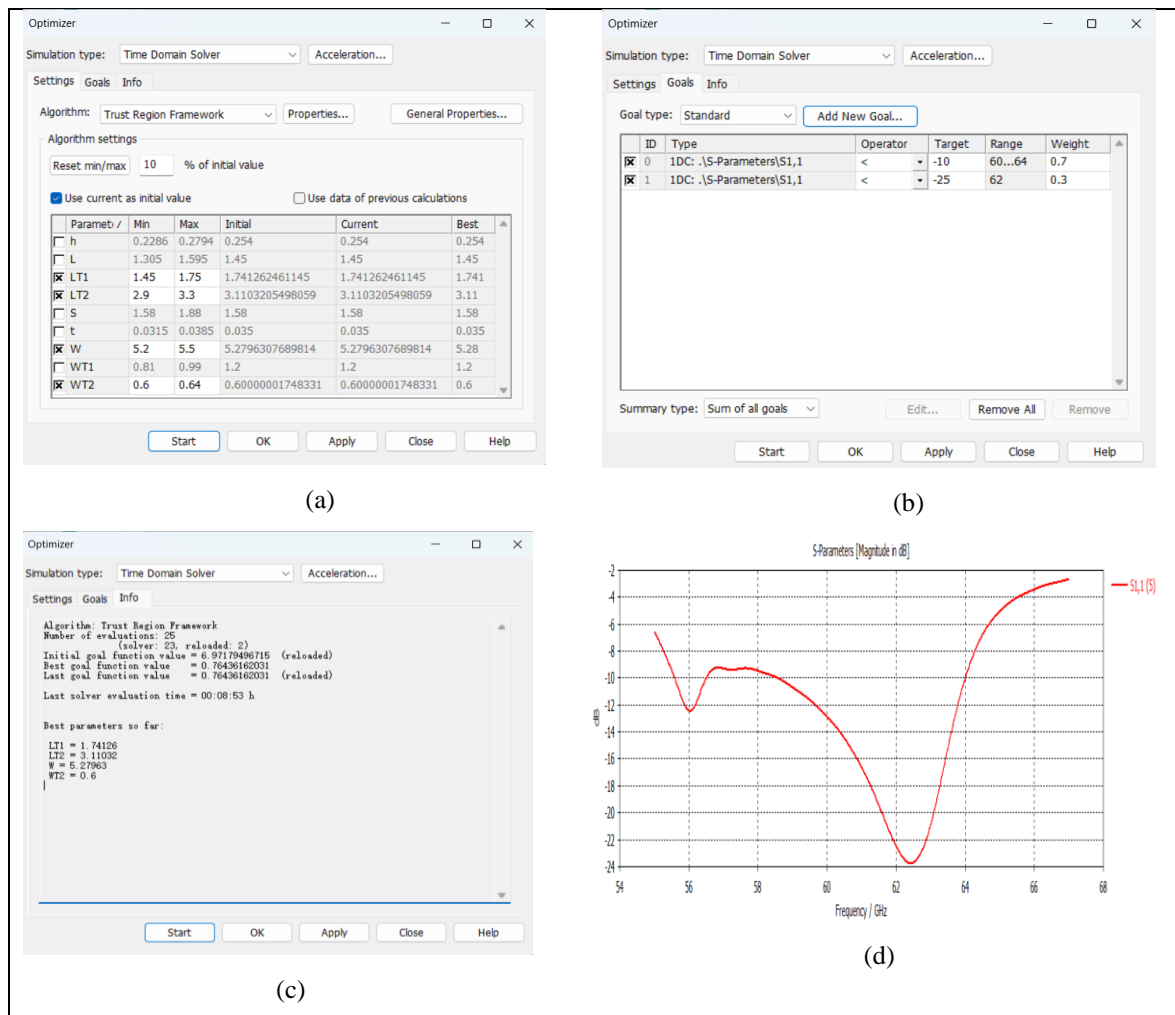
Fig. 15. The process of using optimizer

In addition to the optimizer, parameter sweeper is also an important optimization tool, which can be used to scan a single parameter and observe the effect of this parameter on the S-parameters, the figure below shows the S-parameter resulting from the parameter sweep of WT1:
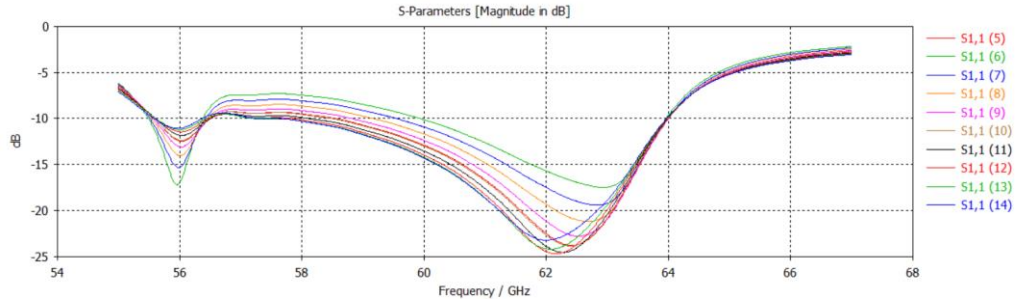

Fig. 16. The process of using parameter sweep

The above is the simulation process and measurement settings of a 3×2 antenna.

Chapter 3

Results & Discussions

3.1   Parameter studies

a) Gain

Antenna gain is the ability of an antenna to radiate in a particular direction relative to an ideal point source. Higher gain indicates that the antenna transmits or receives signals more efficiently in a given direction.

b) S1,1 parameter (Return Loss)

S11 is the reflection coefficient of the antenna, which is usually used to describe the reflection performance of the antenna. The term is determined by quantifying the correlation between the reflected signal at the antenna's input and the input signal. Generally, a lower value of S11 is preferable since it suggests that the antenna has a more favourable match at the intended frequency, resulting in less signal reflection.

c) Directivity

The directionality of an antenna refers to its ability to radiate or receive signals in space. The shape and size of the antenna usually achieve directionality.

d) Beamwidth

Beamwidth refers to the angular width of the antenna's radiation pattern in the main direction of emission. Directional communications typically benefit from narrow beams, but wider beams are more appropriate for broadcasting and covering expansive areas.

e) Impedance

Ensuring efficient energy transfer between the antenna and the transmission line or receiving device heavily depends on the impedance matching of the antenna.

3.2 Parameter lists

a) Antenna arrays with 6 × 1
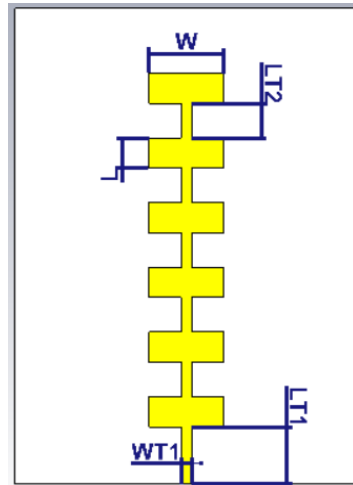
Fig. 17. 6 × 1 antenna arrays

Table. 5. Parameter list of 6×1 antenna

Name	Value(mm)
W	5.10
LT1	4.00
LT2	2.42
WT1	0.50
WT2	0.86
L	2.10

b) Antenna arrays with 3 × 2
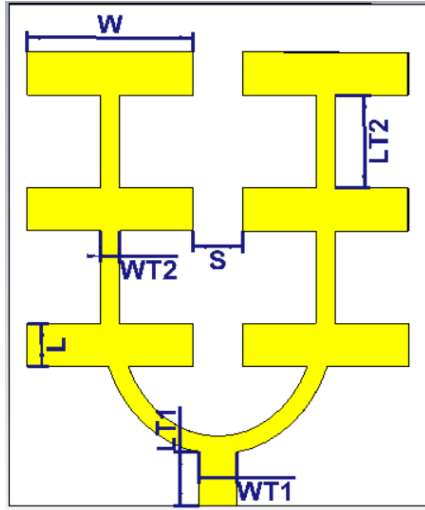
Fig. 18. 3 × 2 antenna arrays

Table. 6. Parameter list of 3×2 antenna

Name	Value(mm)
W	5.28
LT1	1.74
LT2	3.11
S	1.58
WT1	1.2
WT2	0.6
L	1.45

c) Antenna arrays with 6 × 2
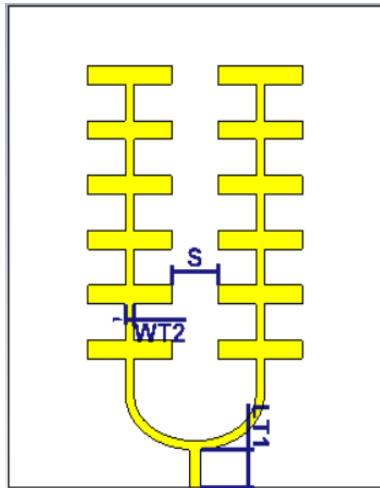
Fig. 19. 6 × 2 antenna arrays
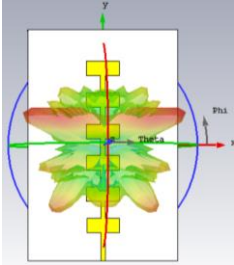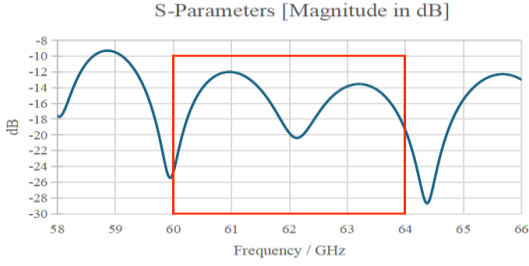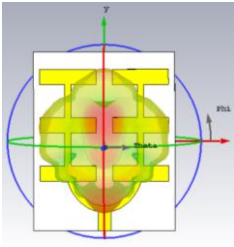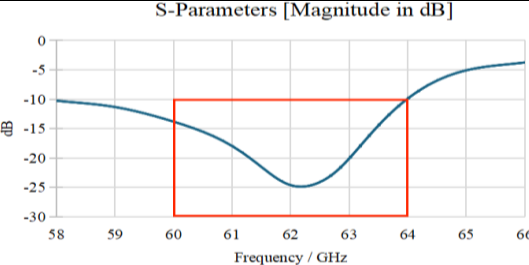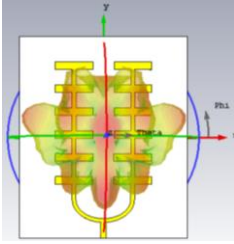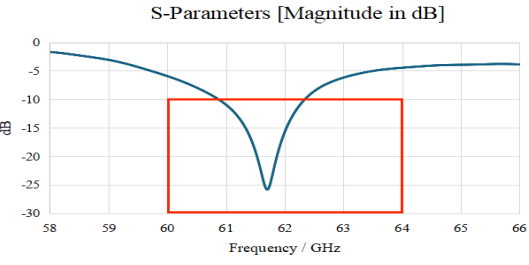
Table. 7. Parameter list of 6×2 antenna

Name	Value(mm)
W	6.22
LT1	3.00
LT2	2.51
WT1	0.87
WT2	0.63
L	1.30

3.3 Preliminary Results

The following table shows the three antennas' structure diagrams, far-field diagrams and S1,1 parameter:

Table. 8. Summary of antenna parameters

	Structure and far-field diagrams	S1,1 parameter	Gain
Ant. 1 (6 × 1)			12.9dBi
Ant. 2 (3 × 2)			13.2dBi
Ant. 3 (6 × 2)			11.2dBi

For 6×1 antenna and 3×2 antenna, their frequency band covers 60-64 GHz, indicating that these antennas have good reflective performance in this frequency band. However, the bandwidth of the 6×1 antenna array is very narrow, covering only 61-62.3 GHz, with a

bandwidth of only about 1.3 GHz. In addition, the 3×2 antenna has the strongest directivity in the z-direction. In contrast, the 6×1 and 6×2 antennas are very directional in the x-direction, which is not the result we want. Furthermore, the 3×2 antenna has the highest antenna gain compared to the other two antennas. Combined with the analysis above, the 3×2 antenna is the most ideal.

3.4   Final Results

Based on the above analysis, we have opted to conduct further research and analysis on a 3x2 antenna array. One antenna will be designated for signal transmission, while the other will serve for signal reception. The antenna diagram illustrating this setup is depicted below. The antenna structure is shown below:
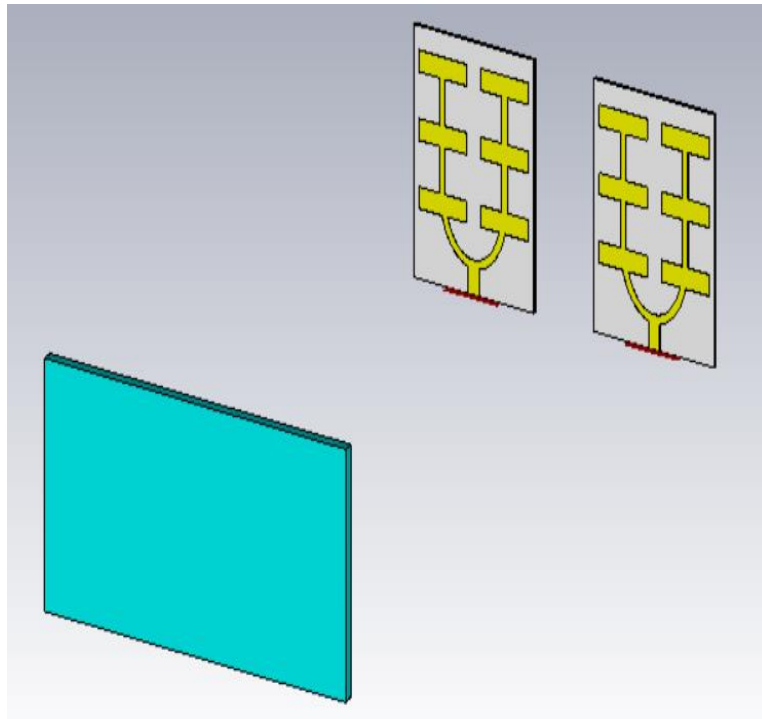
Fig. 20. The final antenna design

In order to observe the performance of the antenna, the distance between the antenna and the copper plate was adjusted using the CST software by increasing the distance from

30mm to 150mm, with an increase of 20mm at a time. Through Fig. 21, it can be observed that the time delay increases with the increase in distance.
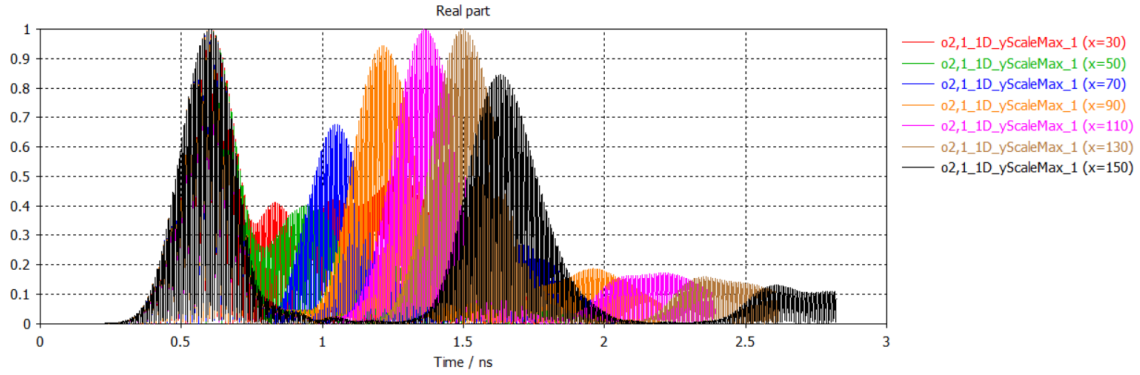
Fig. 21. The time delay

The post-processing allowed us to study the interaction between the antenna and various materials in depth. Three different reflective substrate materials, namely copper, human skin and FR-4, were chosen and placed at a distance of 70 mm from the antenna. It can be noticed that as the dielectric constant of the reflective substrate increases, the magnitude of the signal reflected also increases.
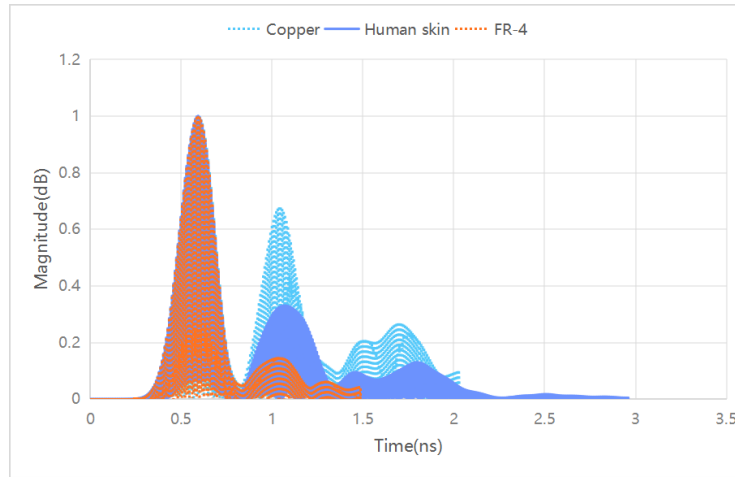
Fig. 22. Magnitude of reflection on different materials

This graph shows the effect of process distance on time delay and amplitude. In the figure, the blue curve indicates a gradual increase in time delay with process distance, with a significant increase reaching a high point, especially after 200 mm. On the other hand, the orange curve depicts the change in amplitude, which first rises to a maximum of 200 mm and then gradually decreases as the distance increases. Also, we can find that the time delay and propagation distance are linearly related.

Fig. 23. Change in time delay and magnitude

Chapter 4

Conclusion and Future Work

4.1 Conclusion

To summarize, this study thoroughly examines the use of ultra-wide patch antenna arrays in the 60 GHz spectrum for monitoring vital signs from a distance. The study involved modelling various configurations of antenna arrays and evaluating the efficiency of both absorbed and transmitted signals in the system design. The main objective was to ensure that the reflection coefficient of the system remains below -10 dB within the 60-64 GHz frequency range. The simulation results were successful for the antenna arrays with 6×1 and 3×2 patch elements, indicating that both antennas have good reflection performance in this frequency band. However, the bandwidth of the 6×1 antenna array is very narrow, covering only 61-62.3 GHz, with a bandwidth of only about 1.3 GHz, and despite the optimization of the antennas using the optimizer and the parameter sweeper, it is still not possible to ensure that the S1,1 parameter is lower than -10 dB in the band of 60-64 GHz. In addition, the 3×2 antenna has the strongest directivity in the z-direction.

In contrast, the 6×1 antenna and the 6×2 antennas have strong directivity in the x-direction, so the 3×2 antenna has better directivity than the other two antennas. Furthermore, for the antenna arrays with 6×1 and 3×2 patch elements, their gains are 12.9dBi,13.2dBi, and 11.2dBi, respectively, and the 3×2 antenna has the highest gain. However, theoretically, the antenna's gain increases with the number of patch elements, whereas the simulation results are the opposite, which requires further study. Combined with the above discussion, we choose the 3×2 antenna for further study. At a later stage of the project, to observe the performance of this antenna, the distance between the antenna and the copper plate was adjusted using the CST software, and the distance was increased from 30 mm to 150 mm, with an increase of 20 mm each time. It can be seen that the time delay increases in a linear relationship with the increase in distance. Afterwards, the

interaction between the antenna and various materials was studied in depth through post-processing. Three different reflective substrate materials, namely copper, human skin and FR-4, were chosen and placed at a distance of 70 mm from the antenna. It can be noticed that the magnitude of the reflected signal increases as the dielectric constant of the reflective substrate increases. Overall, the FYP project is a relative success.
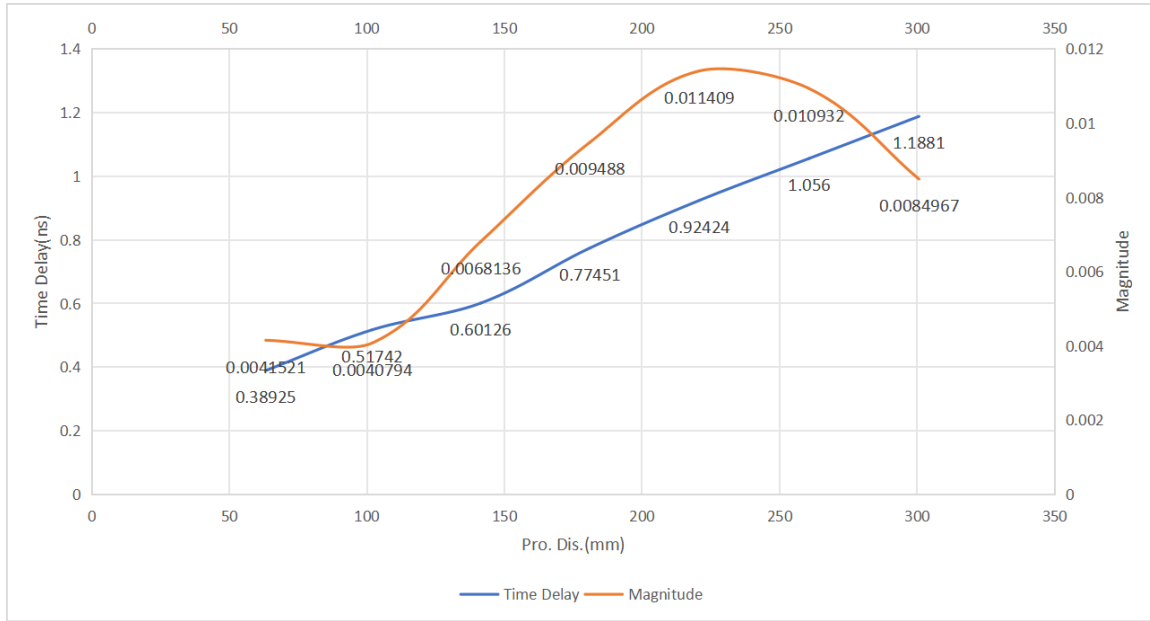
4.2 Future Work

For future research on 64 GHz antenna arrays, two promising directions include:

1) Antenna Fabrication: Future antenna fabrication research should look towards creating new manufacturing methods designed especially for high-frequency applications like 64 GHz. Among these is the application of materials offering superior millimeter-wave frequency bandwidth and radiation efficiency. Another area of emphasis would be the reduction of antenna elements to meet the needs of small devices while ensuring reliable operation in various environments.

2) Dynamic Adjustment of Antenna and Reflector Plate Distance: Future research could look into the effects of dynamically varying the distance between the antenna and the reflector plate because the CST software only enables static settings now. Research might look at how different gap values impact the antenna's gain, general performance, and directional patterns.

References

[1] T. Adiono et al., "Respinos: A Portable Device for Remote Vital Signs Monitoring of COVID-19 Patients," in IEEE Transactions on Biomedical Circuits and Systems, vol. 16, no. 5, pp. 947-961, Oct. 2022, doi: 10.1109/TBCAS.2022.3204632

[2] F. Wang, F. Zhang, C. Wu, B. Wang and K. J. Ray Liu, "ViMo: Vital Sign Monitoring Using Commodity Millimeter Wave Radio," ICASSP 2020 - 2020 IEEE International Conference on Acoustics, Speech and Signal Processing (ICASSP), Barcelona, Spain, 2020, pp. 8304-8308, doi: 10.1109/ICASSP40776.2020.9054152.

[3] G. Duggal, S. Sundar Ram and K. V. Mishra, "Micro-Doppler and Micro-Range Detection via Doppler-resilient 802.11ad-Based Vehicle-to-Pedestrian Radar," 2019 IEEE Radar Conference (RadarConf), Boston, MA, USA, 2019, pp. 1-6, doi: 10.1109/RADAR.2019.8835525.

[4] H-R. Chuang, H-C. Kuo, F-L. Lin, T-H. Huang, C-S. Kuo and Y-W. Ou, 60-GHz millimeter-wave life detection system (MLDS) for noncontact human vital-signal monitoring, IEEE Sensors Journal 12, no. 3 (2012): 602-609.

[5] Y.P. Zhang, M. Sun and L.H. Guo, "On-chip antennas for 60 GHz radios in silicon technology," IEEE Trans. Electron Devices, vol. 52, no. 7, pp.1664-1668, Jul. 2005.

[6] "IEEE Standard for Information technology-- Local and metropolitan area networks-- Specific requirements-- Part 15.3: Amendment 2: Millimeter-wave-based Alternative Physical Layer Extension," in IEEE Std 802.15.3c-2009 (Amendment to IEEE Std 802.15.3-2003), vol., no., pp.1-200, 12 Oct. 2009, doi: 10.1109/IEEESTD.2009.5284444.

[7] Miao Zhang, et al. "Analysis of Intersymbol Interference Characterized by the Large Array Antennas Adopted in a 60-GHz-Band Gigabit Compact-Range Wireless Access System." *IEEE Access*, vol. 9, Jan. 2021, pp. 80077–87. *EBSCOhost*, https://doi.org/10.1109/ACCESS.2021.3084857.

[8] Biglarbegian, B., Fakharzadeh, M., Busuioc, D., *et al.*: 'Optimized microstrip antenna arrays for emerging millimeter-wave wireless applications', *IEEE Trans. Antennas Propag.*, 2011, 59, (5), pp. 1742–1747 (doi: 10.1109/TAP.2011.2123058)

[9] Artemenko, A., Maltsev, A., Mozharovskiy, A., *et al.*: 'Millimeter-wave electronically steerable integrated lens antennas for WLAN/WPAN applications', *IEEE Trans. Antennas Propag.*, 2013, 61, (4), pp. 1665–1671 (doi: 10.1109/TAP.2012.2232266)

[10] Suematsu, N., et al. "A 60-GHz-Band 2 x 4 Planar Dipole Array Antenna Module Fabricated by 3-D SiP Technology." *IOP Conference Series: Materials Science and Engineering*, vol. 61, Jan. 2014. *EBSCOhost*, https://doi.org/10.1088/1757-899X/61/1/012036.

[11] S. Lahmadi and J. B. H. Tahar, "Optimization of 60 GHz MIMO antenna by adding ground stub to reduce mutual coupling for WPAN applications," 2017 25th International Conference on Software, Telecommunications and Computer Networks (SoftCOM), Split, Croatia, 2017, pp. 1-4, doi: 10.23919/SOFTCOM.2017.8115497.

[12] Tomura, T., et al. "8 × 2-Element 60-GHz-Band Circularly Polarized Post-Wall Waveguide Slot Array Antenna Loaded With Dipoles." *IEEE Access, Access, IEEE*, vol. 8, Jan. 2020, pp. 85950–57. *EBSCOhost*, https://doi.org/10.1109/ACCESS.2020.2992922.

[13] M. Ohira, A. Miura and M. Ueba, "60-GHz Wideband Substrate-Integrated-Waveguide Slot Array Using Closely Spaced Elements for Planar Multisector Antenna," in IEEE Transactions on Antennas and Propagation, vol. 58, no. 3, pp. 993-998, March 2010, doi: 10.1109/TAP.2009.2039329.

[14] M. Balle, C. Zhu, B. Zhang, J. Wang, and L. Ran, A 60-GHz Radar Sensor for Micron-Scale Motion Detection[J]. arXiv preprint arXiv:2107.10993, 2021.

[15] L. Sun, Y. Li, H. Hong, F. Xi, W. Cai, X. Zhu, Super-resolution spectral estimation in short-time non-contact vital sign measurement, Review of Scientific Instruments, 2015 Apri1;86(4):044708

[16] A. D. Droitcour, T. B. Seto, B-K. Park, S. Yamada, A. Vergara, C. E. Hourani, T. Shing, A.Yuen, V. M. Lubecke, and O. Boric-Lubecke, Non-contact respiratory rate measurement validation for hospitalized patients, In 2009 Annual International

Conference of the IEEE Engineering in Medicine and Biology Society, pp. 4812-4815. IEEE, (2009)

[17]   M. Villarroel, A. Guazzi, J. Jorge, S. Davis, P. Watkinson, G. Green, A. Shenvi, K. McCormick, and L.Tarassenko, Continuous non-contact vital sign monitoring in neonatal intensive care unit, Healthcare technology letters 1, no. 3 (2014): 87

[18]   S. Suzuki, T. Matsui, M. Kagawa, T. Asao, and K. Kotani, An approach to a non-contact vital sign monitoring using dual-frequency microwave radars for elderly care, Journal of Biomedical Science and Engineering 6, no. 07 (2013): 704

[19]   M. Uenoyama, T. Matsui, K. Yamada, S. Suzuki, B. Takase, S. Suzuki, M. Ishihara, and M. Kawakami, Non-contact respiratory monitoring system using a ceiling-attached microwave antenna, Medical and Biological Engineering and Computing 44, no. 9 (2006): 835-840

[20]   D. Obeid, G. Zaharia, S. Sadek and G. El Zein, 2012. Microwave doppler radar for heartbeat detection vs electrocardiogram. Microwave and Optical Technology Letters, 54(11), pp.2610-2617.

[21]   Kao, T.Y.J. and Lin, J., 2013, April. Vital sign detection using 60-GHz Doppler radar system. In Wireless Symposium (IWS), 2013 I.E. International (pp. 1-4). IEEE.

[22]   C. Gu, Short-Range Noncontact Sensors for Healthcare and Other Emerging Applications: A Review. Sensors, 16(8), 2016, p.1169.

[23]   J. Wang, X. Wang, L. Chen, J. Huangfu, C. Li and L. Ran, "Noncontact Distance and Amplitude Independent Vibration Measurement Based on an Extended DACM Algorithm," in IEEE Transactions on Instrumentation and Measurement, vol. 63, no. 1, pp. 145-153, Jan. 2014, doi: 10.1109/TIM.2013.2277530.

[24]   Q. Lv, T. Hu, S. Qiao, Y. Sun, J. Huangfu and L. Ran, "Non-contact detection of Doppler biosignals based on gradient decent and extended DACM algorithms," 2013 IEEE MTT-S International Microwave Workshop Series on RF and Wireless Technologies for Biomedical and Healthcare Applications (IMWS-BIO), 2013, pp. 1-3, doi: 10.1109/IMWS BIO.2013.6756174.

[25]   T. -J. Tseng and C. -H. Tseng, "Noncontact Wrist Pulse Waveform Detection Using 24-GHz Continuous-Wave Radar Sensor for Blood Pressure Estimation," 2020

IEEE/MTT-S International Microwave Symposium (IMS), 2020, pp. 647-650, doi: 10.1109/IMS30576.2020.9224111.

[26]   M. Mercuri, P. Karsmakers, B. Vanrumste, P. Leroux and D. Schreurs, "Biomedical wireless radar sensor network for indoor emergency situations detection and vital signs monitoring," 2016 IEEE Topical Conference on Biomedical Wireless Technologies, Networks, and Sensing Systems (BioWireleSS), 2016, pp. 32-35, doi: 10.1109/BIOWIRELESS.2016.7445554.

[27]   C. Li, V. M. Lubecke, O. Boric-Lubecke and J. Lin, A review on recent advances in Doppler radar sensors for noncontact healthcare monitoring, IEEE Transactions on microwave theory and techniques 61, no. 5 (2013): 2046-2060

[28]   Bakhtiari, Sasan, Thomas W. Elmer, Nicholas M. Cox, Nachappa Gopalsami, Appostolos C. Raptis, Shaolin Liao, Ilya Mikhelson, and Alan V. Sahakian. BCompact millimeter-wave sensor for remote monitoring of vital signs. IEEE Transactions on Instrumentation and Measurement 61, no. 3 (2012): 830-841.

[29]   S. Bakhtiari, S. Liao, T. Elmer and A. C. Raptis, A real-time heart rate analysis for a remote millimeter wave IQ sensor, IEEE Transactions on Biomedical Engineering 58, no. 6 (2011): 1839-1845

[30]   D. T. Petkie, C. Benton and E. Bryan, Millimeter wave radar for remote measurement of vital signs, (2009): 1.

[31]   Yang, Z., Pathak, P.H., Zeng, Y., Liran, X. and Mohapatra, P., Monitoring Vital Signs Using Millimeter Wave. DOI: http://dx.doi.org/10.1145/2942358.2942381 [Online] Available at: [http://www.phpathak. com/files/mmvital-mobihoc.pdf], accessed on October the 1th, 2016

[32]   T-Y. J. Kao, A. Y-K. Chen, Y. Yan, T-M. Shen and J. Lin, A flip-chip-packaged and fully integrated 60 GHz CMOS micro-radar sensor for heartbeat and mechanical vibration detections, In 2012 I.E. Radio Frequency Integrated Circuits Symposium, pp. 443-446. IEEE, (2012)

Appendix.   MATLAB code for FMCW

```matlab
%% Parameter settings
f_c_start = 60e9; % Start-up frequency: 60 GHz
f_c_end = 64e9; % Upper limit frequency: 64 GHz
T_B = 1e-9; % Scanning time: 1ns
B = f_c_end - f_c_start; % bandwidth
k = 2 * B / T_B; % Sweep Slope
f_s = 50 * f_c_end; % RF sampling rate
T = 2e-9; % RF simulation time
t = linspace(0, T, f_s * T); % time base

%% Waveform generation
f_rf = B * (sawtooth(2 * pi / T_B * t) + 1) / 2 + f_c_start; % time-frequency
characteristic
y = exp(1i * 2 * pi * (f_c_start * t + k * t.^2 / 2)); % Signal Waveform
y_freq = fftshift(fft(y)); % signal spectrum
x_freq = linspace(-f_s / 2, f_s / 2, f_s * T); % signal frequency

%% Plot
figure('NumberTitle', 'off', 'Name', 'FMCW Signal Characteristics', ...
        'Position', [200, 50, 600, 1100], 'PaperPositionMode', 'auto');

% FMCW Time-Frequency Characterisation
subplot(4, 1, 1);
plot(t / 1e-9, f_rf / 1e9, 'r-');
xlabel('Time/ns');
ylabel('Frequency/GHz');
title('Linear Frequency Modulation Characteristic');
set(gca, 'FontName', 'Arial', 'FontSize', 11);
grid on;
ylim([f_c_start / 1e9 f_c_end / 1e9]);

% Time domain waveform (real part, cosine)
subplot(4, 1, 2);
plot(t / 1e-9, real(y), 'r-');
xlim([0 2]);
xlabel('Time/ns');
ylabel('Amplitude');
title('Time Domain Waveform - Real Part (Zoomed up in time axis)');
set(gca, 'FontName', 'Arial', 'FontSize', 11);
grid on;

% Write to ASCII file
y_file = real(y);
fid = fopen('signal.txt', 'wt');
fprintf(fid, '%1.13f, %1.5f\n', [t; y_file]);
```

32

```matlab
fclose(fid);

% Time domain waveform (imaginary part, sine)
subplot(4, 1, 3);
plot(t / 1e-9, imag(y), 'r-');
xlim([0 2]);
xlabel('Time/ns');
ylabel('Amplitude');
title('Time Domain Waveform - Imaginary Part (Zoomed up in time axis)');
set(gca, 'FontName', 'Arial', 'FontSize', 11);
grid on;

% Signal spectrum
subplot(4, 1, 4);
plot(x_freq / 1e9, abs(y_freq) / max(abs(y_freq)), 'r-');
xlim([55 80]);
xlabel('Frequency/GHz');
ylabel('Normalized Magnitude');
title('Frequency Spectrum');
set(gca, 'FontName', 'Arial', 'FontSize', 11);
grid on;

% Adjust subplot positions
left_start = 0.11;
bottom_start = 0.06;
sub_wid = 0.86;
sub_hig = 0.17;
sub_ver_step = 0.25;
for i = 1:4
    axes_name = subplot(4, 1, i);
    set(axes_name, 'Position', [left_start, bottom_start + (4 - i) *
sub_ver_step, sub_wid, sub_hig]);
end
```